Binding of Cationic Single-Chain and Dimeric Surfactants to Bovine Serum Albumin

ARTICLE *in* LANGMUIR · MAY 2013

Impact Factor: 4.46 · DOI: 10.1021/la400789k · Source: PubMed

Langmuir

Article

pubs.acs.org/Langmuir

Binding of Cationic Single-Chain and Dimeric Surfactants to Bovine Serum Albumin

Victoria Isabel Martín, Amalia Rodríguez, Alfredo Maestre, and María Luisa Moyá*

Department of Physical Chemistry, University of Seville, C/Profesor García González 1, 41012 Seville, Spain

Supporting Information

ABSTRACT: The interactions between bovine serum albumin (BSA) and the single-chain surfactants *N*-benzyl-*N*,*N*-dimethyl-*N*-(1-dodecyl)-ammonium bromide (PH12) and *N*-cyclohexylmethyl-*N*,*N*-dimethyl-*N*-(1-dodecyl)ammonium bromide (CH12) and their two dimeric counterparts, *N*,*N*′-[1,3-phenylenebis(methylene)]bis[*N*,*N*-dimethyl-*N*-(1-dodecyl)]-ammonium dibromide (12PH12) and *N*,*N*′-[cyclohexane-1,3-diylbis-(methylene)]bis[*N*,*N*-dimethyl-*N*-(1-dodecyl)]ammonium dibromide (12CH12), respectively, have been investigated by surface tension, fluorescence, circular dichroism, ζ potential, and atomic force microscopy. The results obtained permit the examination of the way an increase in the number of hydrophobic chains and the substitution of a cyclohexyl ring by a phenyl ring, either in the headgroup of single-chain surfactants or in the spacer of dimeric surfactants, affect BSA−surfactant interactions. The comparison of the fluorescence results with those obtained by ζ potential measurements shows that the sites of binding of the surfactants with aromatic rings to the BSA are somewhat different from those of the surfactants with no aromatic rings.

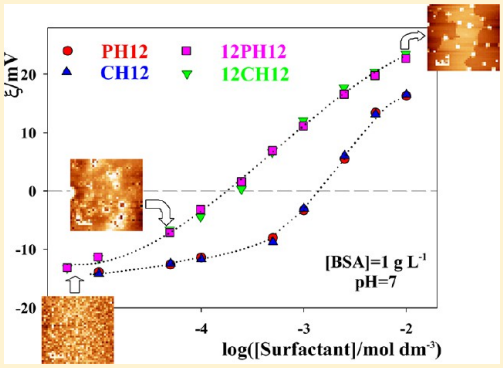

INTRODUCTION

Proteins are important in living organisms and take part in many life processes. They can bind a wide variety of ligands such as bilirubin, fatty acids, hematin, metal ions, drugs, and surfactants.[1−5] Interactions of proteins with surfactants have been extensively studied because their mixtures have important applications in biosciences, foods and cosmetics, drug delivery, detergents, and biotechnological processes.[6−10] It has been established that the developing protein−surfactant interaction may alter the original functional properties of the protein. This means that not only the solubility or the aggregation properties but also the conformational parameters of the protein may be modified.

Protein−surfactant interactions are usually dependent on the surfactant features. Most of the research has been focused on single-chain surfactants.[11−13] More recently, the binding between proteins and dimeric surfactants has been discussed.[14−18] These surfactants consist of two hydrophobic chains and two polar headgroups covalently linked through a spacer group, which influences their properties significantly. They have unique aggregation properties such as a lower critical micelle concentration (cmc) and Kraft temperature, special aggregation morphology, strong hydrophobic microdomains, etc.[19,20] Various applications of dimeric surfactants, relevant to the surfactant−protein interactions, viz., antimicrobial, hair conditioning, skin and eye care, etc., are superior to those of conventional surfactants.[21,22]

Our research group has recently prepared and characterized the two single-chain surfactants *N*-benzyl-*N*,*N*-dimethyl-*N*-(1-dodecyl)ammonium bromide (PH12) and *N*-cyclohexylmethyl-*N*,*N*-dimethyl-*N*-(1-dodecyl)ammonium bromide (CH12) and their two dimeric counterparts, *N*,*N*′-[1,3-phenylenebis-(methylene)]bis[*N*,*N*-dimethyl-*N*-(1-dodecyl)]ammonium dibromide (12PH12) and *N*,*N*′-[cyclohexane-1,3-diylbis-(methylene)]bis[*N*,*N*-dimethyl-*N*-(1-dodecyl)]ammonium dibromide (12CH12), respectively.[23] The study of the binding of these surfactants to proteins could provide information about the influence of various factors on protein−surfactant interactions: (i) an increase in the number of hydrophobic chains, (ii) changes in the headgroup by substituting a cyclohexyl ring by a phenyl ring, and (iii) changes in the spacer of dimeric surfactants by substituting a cyclohexyl ring with a phenyl ring. With regard to proteins, bovine serum albumin (BSA) is one of the most extensively studied serum albumins. Besides, BSA and human serum albumin, which is an important transfer protein, are approximately 76% homologous and display a strictly conserved repeating pattern of disulfides.[24] Therefore, study of the behavior of surfactants in the presence of BSA can contribute to pharmacokinetics and pharmacodynamics. In this work, interactions of PH12, CH12, 12PH12, and 12CH12 with BSA were investigated by using surface tension, fluorescence, circular dichroism, ζ potential, and atomic force microscopy. When necessary, interactions of BSA with other surfactants were also investigated to help the

Received: March 1, 2013
Revised: April 28, 2013
Published: May 24, 2013

   dx.doi.org/10.1021/la400789k | Langmuir 2013, 29, 7629−7641

Scheme 1

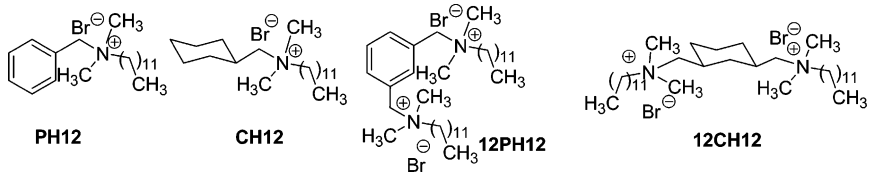

discussion. The studies proposed in this work would contribute to a better understanding of the role of the molecular structures of surfactants in surfactant−protein interactions and, therefore, in the behavior of surfactants as denaturants.

EXPERIMENTAL SECTION

Materials. BSA was from Aldrich and was used without further purification. Buffer salts and $MgCl_2$ were purchased from Aldrich. Dodecyltrimethylammonium bromide (DTAB), hexadecyltrimethylammonium chloride (CTAC), and benzyldimethylhexadecylammonium chloride (BDHC) were also from Aldrich. Dodecyltriphenylphosphonium bromide (TPB) was from Lancaster. 8-Anilinonaphthalene sulfonate (ANS) was obtained from Fluka and used as received. Doubly distilled water was used in all the experiments.

The syntheses of the surfactants (see Scheme 1) were conducted as described in ref 23.

Surface Tension Measurements. Surface tensions were measured by a du Noüy ring method using a KSV 703 digital tensiometer (Finland) equipped with an automatic device to set the time between two consecutive measurements and to select the rising velocity of the platinum ring. A water-jacketed sample beaker connected to a cryostat was used to control the sample temperature. Prior to each measurement, the ring was rinsed with ethanol and then heated briefly by being held above a Bunsen burner until it glowed. The vessel was cleaned by using chromic sulfuric acid, boiled in distilled water, and then flamed with a Bunsen burner before use. The precision in the measurements was ±1 mN m^{-1}. Care has to be taken in using the du Noüy ring method to deduce surfactant properties, because the surfactant adsorption kinetics can influence the results.[26,27] In our experiments, the ring rising velocity was set sufficiently low to allow the surfactant adsorption to reach equilibrium. This was particularly important when the surface tension of dimeric surfactant solutions was measured.

Fluorescence Measurements. Fluorescence measurements were taken by using a Hitachi F-2500 fluorescence spectrophotometer. The temperature was kept at 303 K by a water flow cryostat connected to the cell compartment.

To investigate the effect of surfactant addition on the intrinsic fluorescence of BSA, fluorescence spectra of solutions containing a fixed BSA concentration (0.33 g/L) and different surfactant concentrations were recorded with a 1 cm path length cell. The excitation and emission slits were set at 2.5 nm. The reference sample consisting of the buffer and the surfactant was checked for fluorescence signals. The solution was excited at 280 nm, and the emission spectra were recorded within the range of 290−450 nm.

The synchronous fluorescence spectra of solutions containing a fixed BSA concentration (0.33 g/L) and increasing surfactant concentrations were recorded by keeping the $\Delta\lambda$ between the excitation and emission wavelengths equal to 20 and 60 nm, respectively. In this way, the spectra provide information about how the surfactant concentration affects the contribution to the BSA fluorescence emission of tyrosine and tryptophan residues, respectively.[28]

Fluorescence emission of ANS in the presence of BSA was studied by recording the emission spectra of solutions containing a fixed BSA concentration (0.33 g/L) and varying ANS concentrations. The excitation wavelength was 355 nm, and the excitation and emission slits were 2.5 nm. Subsequently, the effect of the addition of surfactant on the ANS fluorescence was investigated by monitoring the fluorescence emission of solutions containing fixed protein (0.33 g/L) and ANS (2×10^{-5} mol dm^{-3}) concentrations and increasing the surfactant concentration.

Circular Dichroism. Circular dichroism (CD) experiments were performed in a Biologic Mos-450 spectropolarimeter. A circulation thermostatic bath kept the sample temperature at 303 K. All spectra were corrected for background by subtraction of appropriate blanks. A cuvette with a 0.1 cm path length was used, and the spectra were recorded within the range from 160 to 335 nm, with a slit width of 1 nm and a scan speed of 50 nm min^{-1}. Argon was passed through the solutions for >2 h. The reported spectra were the average of five scans. No contribution from the buffer or the surfactants to the CD spectra was found. Data are represented as molar ellipticities, θ, which were calculated by using the equation $\theta = \theta_{obs}/(10CL)$, where θ_{obs} is the observed ellipticity (in millidegrees), C is the protein molar concentration, and L is the path length in centimeters.

ζ Potential Measurements. ζ potential experiments were taken with a Zetasizer Nano ZS from Malvern Instrument Ltd., which measures the electrophoretic mobility of the sample from the velocity of the particles using a laser doppler velocimeter (LVD). The apparatus is in the General Research Services of the University of Seville (CITIUS). A DTS1060 polycarbonate capillary cell was used at 303 K. The ζ potential (millivolts) of BSA as a function of surfactant concentration was measured. A protein concentration of 1.0 g/L was used. At this BSA concentration, the quality of the signal was good and the standard deviation of the measurements remained low. Six ζ potential measurements were taken at each surfactant concentration, and the average value (standard deviation) was considered.

Atomic Force Microcospy (AFM). The images were obtained with a Molecular Imaging PicoPlus 2500 AFM instrument (Agilent Technologies). The apparatus is in the General Research Services of the University of Seville (CITIUS). Cantilevers (model PPP-FMR-20, Nanosensor) with a resonance frequency within the range of 45−115 Hz were used. All AFM imaging was conducted in air and in tapping mode, with scan speeds of ∼0.5 Hz and data collection at 256 × 256 pixels. AFM images were obtained by drying 30 μL of the working solution (pH 7), deposited on a freshly cleaved mica surface, adsorbed for 30 min, and the surface was washed with doubly distilled water and then air-dried. For some of the working solutions (see below), the mica surface had to be modified for the species present in the solution to be adsorbed. To do this, 30 μL of 0.01 mol dm^{-3} $MgCl_2$ was dropped onto a freshly cleaved mica surface and incubated for 20 min and the surface was washed with doubly distilled water. Subsequently, the same procedure described above was followed.

The experimental results were treated with WSxM 4.0 Beta 6.2 from Nanotec.[29]

In all the experiments, BSA solutions were freshly prepared in 0.01 mol dm^{-3} sodium phosphate buffer (ionic strength of 0.0108 mol dm^{-3}) at pH 7.

RESULTS AND DISCUSSION

Before we discuss the results obtained in this work, relevant information about the micellization process of the surfactants in aqueous solution is required. Table 1 summarizes this information. Table 1 shows that the cmc of CH12 is lower than that of PH12. This result could be explained by considering the conformational freedom of the cyclohexyl ring, when compared to that of the rigid phenyl ring. It is also interesting to point out that ^{1}H NMR two-dimensional (2D) rotating frame nuclear Overhauser effect spectroscopy measure-

dx.doi.org/10.1021/la400789k | Langmuir 2013, 29, 7629−7641

Table 1. Critical Micelle Concentrations, Degrees of Micellar Ionization (α), Average Aggregation Numbers (N_{agg}), and Gibbs Energies of Micellization ($\Delta G°_M$) for the Single-Chain and Dimeric Surfactants Studied at 303 K[a]

surfactant	cmc ($\times 10^3$ mol dm^{-3})	α	N_{agg}	$\Delta G°_M$ (kJ mol^{-1})
PH12	5.8	0.30	32[b] (37)[c]	−38.6
CH12	4.7	0.36	27[b] (34)[c]	−38.1
12PH12	0.97	0.25	18[b] (25)[c]	−47.5
12CH12	1.0	0.32	16[b] (22)[c]	−45.4

[a]Data taken from ref 23. [b]Obtained by steady state fluorescence quenching. [c]Obtained by time-resolved fluorescence quenching.

Table 2. Experimental C_1 Values, Surface Excess Concentrations (Γ_{exc}), and Minimal Surface Areas per Molecule (A_{min}) for BSA/Surfactant Solutions at pH 7 and 303 K[a]

surfactant	C_1 ($\times 10^3$ mol dm^{-3})	Γ_{exc} ($\times 10^6$ mol m^{-2})	A_{min} ($\times 10^{19}$ m^2)
PH12	3.4	1.4 (3.4)	12 (4.8)
CH12	2.1	1.9 (3.6)	9.0 (3.1)
12PH12	1.0	0.48 (1.5)	35 (11)
12CH12	1.0	0.52 (1.1)	32 (15)

[a]Values in parentheses correspond to the buffered surfactant solutions in the absence of protein.

ments (ROESY) show that within the micellar aggregates the phenyl and cyclohexyl rings of the surfactants are bent toward the micellar interior to avoid contact with water.

Tensiometry. Figure 1 shows the dependence of surface tension, γ, on ln[surfactant] for the buffered surfactant solutions (0.01 mol dm^{-3} phosphate buffer) in the absence and presence of BSA (0.33 g/L). In the absence of protein, a well-defined break point is observed, corresponding to the cmc. It is worth noting that the surface tension of the buffer solution containing BSA is lower than that of pure buffer because of the surface active nature of BSA.[30] The γ versus ln[surfactant] curves in the presence of BSA exhibit one break point, C_1, which marks the concentration above which the aggregation of surfactants occurs.[31] The C_1 values are summarized in Table 2. At pH 7, BSA has a negative charge.[32] At low surfactant concentrations, the interaction between the protein and the cationic surfactants at the interface is expected to be dominated by electrostatic interactions,[17] and then protein interacts with surfactants via hydrophobic forces as the surfactant concentration increases. The diminution in γ with an increasing surfactant concentration would be caused by the formation of protein−surfactant complexes of enhanced surface activity compared to that of the native protein.

The slope of the initial linear decrease in γ with an increasing surfactant concentration is a measure of the interfacial adsorption efficacy of the surfactant, which can be quantified by the Gibbs surface excess concentration, Γ_{exc}. To calculate Γ_{exc}, the Gibbs equation will be used:

$$\Gamma_{exc} = -\frac{1}{nRT}\left[\frac{d\gamma}{d(\ln[\text{surfactant}])}\right] \quad (1)$$

where R and T have their usual meaning and n is a constant that depends on the number of species constituting the surfactant and are adsorbed at the interface. Because surface tension

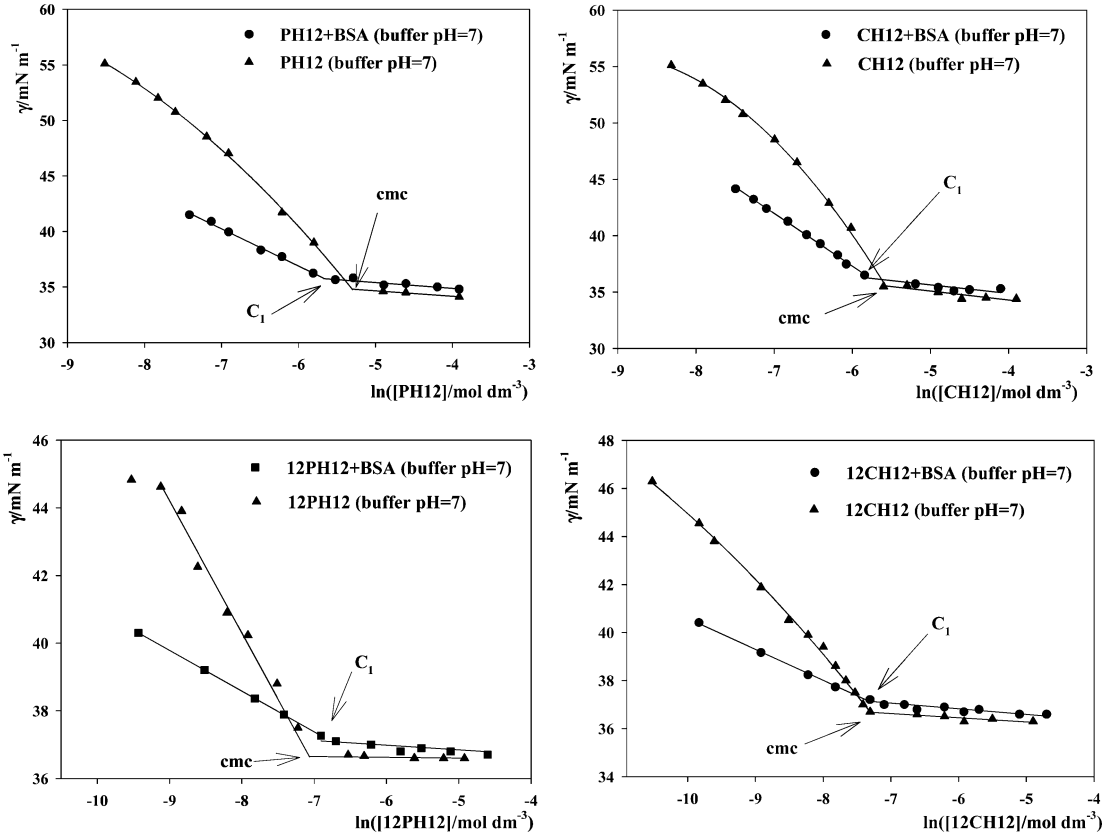

Figure 1. Dependence of the surface tension, γ, on ln[surfactant] in buffered surfactant solutions (pH 7) in the presence and absence of protein at 0.33 g/L BSA and 303 K.

dx.doi.org/10.1021/la400789k | Langmuir 2013, 29, 7629−7641

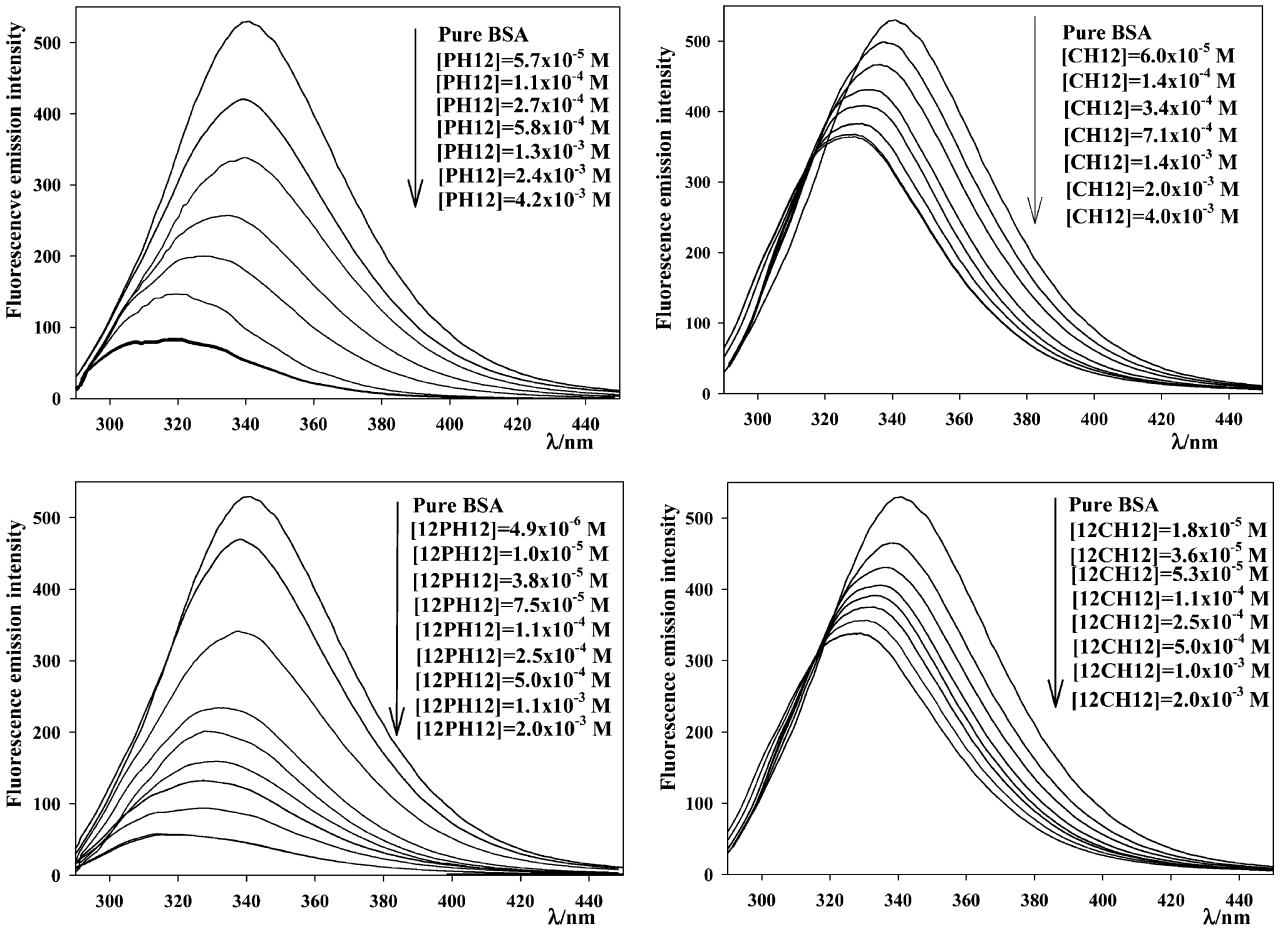

Figure 2. Emission spectra of BSA (0.33 g/L) in the presence of various surfactant concentrations (λ_{exc} = 280 nm) at pH 7 and 303 K.

measurements were taken in 0.010 mol dm^{-3} phosphate buffer, n will be taken to be 1 for all the surfactant solutions studied. The possible contribution of the counterions and buffer ions has not been considered, as they have no preference for interfacial adsorption. From Γ_{exc}, the minimal surface area per molecule, A_{min}, can be estimated by using the expression $A_{min} = (N_A\Gamma_{exc})^{-1}$, where N_A is Avogadro's number. The values of the surface excess concentration and minimal surface area per molecule at the interface are listed in Table 2 for buffered surfactant solutions in the absence and presence of BSA. There are some limitations in the use of eq 1, mentioned by Thomas et al. and Eastoe et al.,[33−36] but they would not affect the qualitative discussion of the data summarized in Table 2.

The observed Γ_{exc}(surfactant) > Γ_{exc}(surfactant+protein) relation and the consequent A_{min}(surfactant) < A_{min}(surfactant +protein) relation can be explained by the reduced compactness of the interfacial monolayer at the air−solution interface in the presence of BSA, which comes from the presence of the solubilized protein−surfactant complexes at the interfacial monolayer.[31]

Intrinsic Fluorescence from BSA. Protein conformation, dynamics, and intermolecular interactions can be investigated through the study of the fluorescence of the aromatic amino acids [tryptophan (Trp), tyrosine (Tyr), and phenylalanine (Phe)], which operate as intrinsic fluorescence probes.[37] The intrinsic fluorescence of BSA is essentially caused by the Trp and Tyr residues. BSA has 18 Tyr residues in different domains of the protein, although they are in abundance in subdomain IC of domain I and subdomain IIC of domain II as compared to other subdomains. The two Trp residues contribute greatly to the intrinsic fluorescence of BSA (below). The Trp located in domain I, subdomain IC, is buried in a hydrophobic pocket and lies near the surface of the albumin molecule. The Trp located in domain II, subdomain IIA, resides in a hydrophobic cavity of the protein. By excitation at 280 nm, where both Trp and Tyr residues become excited, the changes in the wavelength of the emission maximum (a parameter sensitive to protein conformation) and fluorescence intensities can be used to investigate protein−surfactant interactions. Figure 2 shows the variations in the emission spectra of 0.33 g/L BSA buffered solutions, when excited at 280 nm, with a changing surfactant concentration. It is worth noting that buffered solutions of CH12 and 12CH12 show negligible fluorescence. In the case of PH12 and 12PH12, the fluorescence spectra of BSA were corrected, when necessary, from the fluorescence contribution of the surfactant. Figure 2 shows that, for all the surfactants studied, an increase in surfactant concentration results in a blue shift of the emission maximum as well as in a decrease in fluorescence intensity. These changes suggested a shift of the fluorophores to a more hydrophobic environment, which can be explained by considering the binding of the surfactant molecules to the protein, thus screening the fluorophores from the polar solvent. Figure 2 shows that λ_{max} and the fluorescence emission intensity remain approximately constant for surfactant concentrations close to or somewhat higher than C_1 (there is an overlap of the spectra corresponding to the two more concentrated surfactant solutions). That is, saturation of the binding of the surfactant to the protein is observed.

dx.doi.org/10.1021/la400789k | Langmuir 2013, 29, 7629−7641

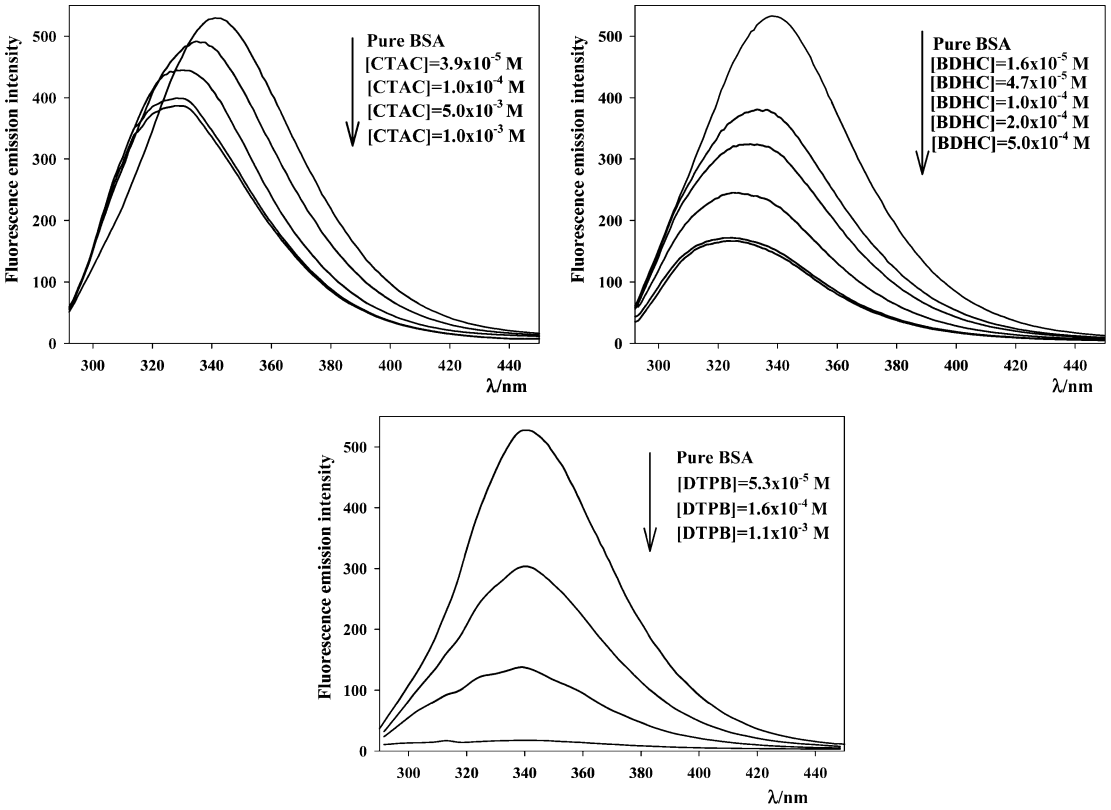

Figure 3. Emission spectra of BSA in the presence of various surfactant concentrations of CTAC, BDHC, and DTPB at 0.33 g/L BSA, pH 7, and 303 K.

Figure 2 shows that an increase in the number of hydrophobic chains in the surfactant as well as the substitution of a cyclohexyl ring with a phenyl ring, either in the headgroup of the single-chain surfactants or in the spacer of the dimeric surfactants, results in a larger diminution of the intrinsic BSA fluorescence intensity. At the working pH, BSA has a negative charge[32,38] and the interactions between the surfactants and the protein are electrostatic as well as hydrophobic. In the case of the surfactants investigated, both interactions are expected to be stronger for dimeric than for single-chain surfactants. This agrees with the stronger effect on the BSA fluorescence emission caused by the former versus the latter. With regard to the influence of the ring nature, surfactants with a phenyl ring can interact through $\pi-\pi$ interactions with protein residues with aromatic rings, such as Trp and Tyr. This would favor the surfactant binding to BSA, and as a result, a stronger effect on the intrinsic fluorescence of BSA would be observed.

With the scope of further investigating the effect of the presence of aromatic rings in the surfactant on protein−surfactant interactions, fluorescence measurements were taken in both BSA with hexadecyltrimethylammonium chloride (CTAC) and BSA with benzyldimethylhexadecylammonium chloride (BDHC) solutions. The only distinction between BDHC and CTAC is BHDC has one benzyl ring and two -CH_3 groups in the headgroup and CTAC has three -CH_3 groups. Therefore, the differences in the influence of these surfactants on the BSA fluorescence emission would come from the presence of the benzyl ring. The critical micellar concentrations of BHDC and CTAC at 303 K are 5.0×10^{-4} mol dm^{-3} (ref 39) and 1.3×10^{-3} mol dm^{-3} (ref 40), respectively. Figure 3 shows the results of this study. One can see that CTAC is less effective than BDHC in diminishing the fluorescence emission of BSA, as was expected because CTAC can interact with BSA through electrostatic and hydrophobic interactions, whereas for BDHC, $\pi-\pi$ interactions can be operative too.

The emission fluorescence spectra of BSA were also registered in the presence of dodecyltriphenylphosphonium bromide (DTPB) [cmc of pure DTPB of 2.0×10^{-3} mol dm^{-3} (ref 41)]. DTPB has a dodecyl hydrophobic chain and a phosphonium headgroup with three phenyl rings. In spite of having a phosphonium instead of an ammonium in the headgroup, some information about the effects caused by the aromatic rings on the BSA intrinsic fluorescence can be obtained. The results are included in Figure 3, and they show that a DTPB concentration of 1.1×10^{-3} mol dm^{-3} practically quenched the intrinsic fluorescence of the protein. Therefore, the experimental results indicate that the presence of aromatic rings in the headgroup of single-chain surfactants results in a more efficient quenching of the intrinsic fluorescence of BSA.

The influence of the presence of aromatic rings in the spacer of dimeric surfactants on surfactant−BSA interactions was also investigated. Li et al.[42] studied the interaction of the dimeric alkanedyil-α,ω-(dodecyldimethylammonium bromide), 12-s-12,2Br$^-$, cationic surfactants (with 2, 3, and 12 methylenes in the spacer) with BSA. The effects of surfactant concentration on the protein emission were similar to those found in this work for 12CH12. On the other hand, Zhou et al.[43] investigated the interactions of dimeric imidazolinium surfactants with BSA and found that, comparing their results with those found for 12-2-12,2Br$^-$, the presence of the imidazolinium ring results in a stronger diminution of the intrinsic fluorescence of BSA. The explanation would be the same as that given for single-chain surfactants. The presence of aromatic rings in the spacer permits $\pi-\pi$ interactions between

dx.doi.org/10.1021/la400789k | Langmuir 2013, 29, 7629−7641

protein residues with aromatic rings and surfactants to be operative. This would result in a stronger effect on BSA fluorescence emission.

The dependence of the average number, υ, of surfactant molecules bound to a BSA molecule can provide information about the type of BSA−surfactant binding.[44] υ was estimated by using the equation $\upsilon = \alpha(C_S/C_{BSA})$, where C_S and C_{BSA} are the molar surfactant concentration and the molar protein concentration, respectively, and α can be estimated from the equation[45]

$$\alpha = \frac{I_{obs} - I_o}{I_{min} - I_o} \quad (2)$$

where I_{obs} is the BSA fluorescence intensity at any surfactant concentration, I_o is the BSA fluorescence intensity in the absence of surfactant, and I_{min} is the minimal BSA fluorescence intensity observed in the presence of surfactant. Figure 4 shows

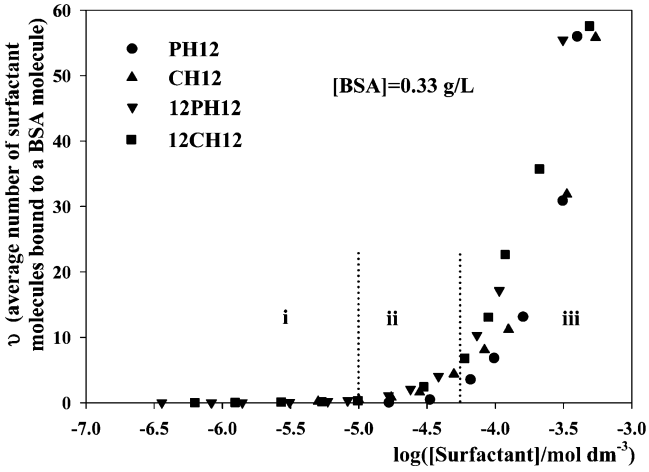

Figure 4. Binding curve of the surfactants with BSA at pH 7 and 303 K.

the dependence of υ on log[surfactant] for the protein−surfactant systems studied up to ~5×10^{-4} mol dm^{-3}. In this figure, three characteristic regions can be distinguished.[8] In the first region (i), at very low surfactant concentrations, there is some binding to specific high-energy sites of the protein. This region is followed by a slow rising part (ii), where a binding of noncooperative character occurs. The third region (iii) is characterized by a massive increase in the level of binding due to cooperative interactions. As mentioned above, there is a fourth region, at higher surfactant concentrations corresponding to the binding saturation. In this region, the addition of more surfactant results in the formation of aggregates. Figure 4 shows that all four surfactants studied bind to BSA in a cooperative manner.

Synchronous Fluorescence of BSA. Synchronous fluorescence, in comparison with conventional fluorescence spectroscopy, is preferable for the analysis of complex multicomponent samples. It reduces spectral overlaps by narrowing spectral bands and simplified spectra by using a suitable wavelength interval.[46] When $\Delta\lambda$ between the excitation wavelength and emission wavelength was kept at 20 or 60 nm, the synchronous fluorescence gives information about Tyr or Trp residues, respectively.[46] Therefore, the study of changes in the synchronous spectra of the protein−surfactant systems with a change in surfactant concentration can provide information about the interaction of the surfactants with the BSA fluorophores, or regions in their vicinity. Figure 5 shows the synchronous spectra of BSA in the presence of several surfactant concentrations. One can see that the Trp residues contribute considerably more to the intrinsic fluorescence of BSA than Tyr residues, because the fluorescence intensity at 60 nm is higher than that at 20 nm. The synchronous spectra of PH12 and 12PH12 in the absence of protein were investigated. No contribution to the spectra with a $\Delta\lambda$ of 60 nm was observed within the wavelength range considered. However, for a $\Delta\lambda$ of 20 nm, the band centered at 265 nm is caused by the emission of these surfactants.

Figure 5 shows that all surfactants interact with both the Trp and Tyr residues or in their vicinity, although from the larger variations in the fluorescence emission of Trp, a greater affinity of the surfactants for this fluorophore or its surroundings is observed. The increase in the number of hydrophobic chains and the presence of the phenyl ring augment the efficacy of the surfactants in diminishing the fluorophore emission, in agreement with the results shown in Figure 2.

Fluorescence of an External Probe (ANS). The photophysical properties of ANS are complex. It absorbs in the near UV with two characteristic maxima at 352 and 375 nm. The emission of ANS arises from two different excited states. In nonpolar solvents, the excited state, localized on the naphthalene ring, emits around 470 nm, showing small changes with polarity. In polar solvents (e.g., methanol and ethanol), the initially excited state undergoes an intramolecular electron transfer reaction forming a charge transfer state that emits at longer wavelengths displaying a higher sensitivity to the polarity of the solvent. In aqueous solutions, an intermolecular electron transfer reaction with solvent occurs, deactivating the charge transfer state and thus decreasing its fluorescence quantum yield.[47] ANS is widely used in protein studies.[31] It can bind to native and partially unfolded proteins. The binding of ANS to BSA was recently investigated by Cattoni et al.[25] These authors showed that three ANS molecules are bound at hydrophobic cavities in BSA subdomains IIA and IIIA and three additional ANS molecules are bound to water-exposed sites. The fluorescent features of ANS, a blue shift of the maximal emission wavelength and an increase in the quantum yield and lifetime, when it is transferred from water to proteins are generally attributed to the binding at hydrophobic sites where, additionally, its mobility is restricted. The ANS molecules bound to the water-exposed sites show low quantum yields.[48] It is known that ANS competes with other protein ligands, such as surfactants, for the binding sites. Besides, ANS fluorescence is sensitive to alterations in protein structure. For these reasons, the fluorimetric study of the binding of ANS to BSA in the presence of surfactants can provide information about BSA−surfactant interactions.

The BSA−ANS system, in the absence of surfactant, was studied by keeping constant the protein concentration (0.33 g/L) and varying the ANS concentration (see Figure 1A of the Supporting Information). Subsequently, in the presence of constant BSA (0.33 g/L) and ANS (2×10^{-5} mol dm^{-3}) concentrations, the influence of an increase in surfactant concentration on the ANS fluorescence intensity was investigated (see Figure 2A of the Supporting Information). Figure 6 shows the dependence of the I/I_o ratio on the surfactant concentration, I and I_o being the protein-bound ANS fluorescence intensity in the presence and absence of surfactant

dx.doi.org/10.1021/la400789k | Langmuir 2013, 29, 7629−7641

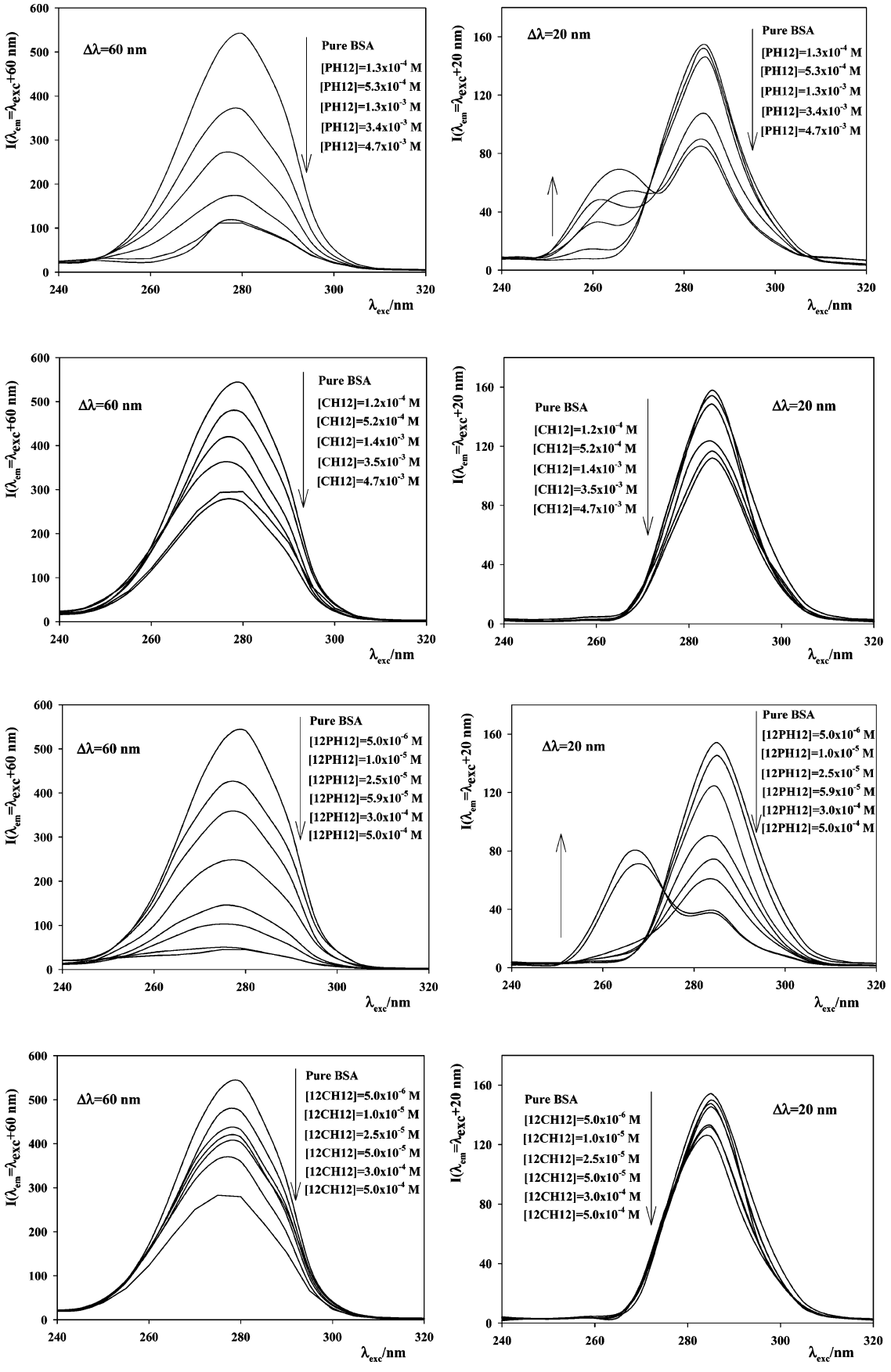

Figure 5. Synchronous spectra of BSA−surfactant systems at 0.33 g/L BSA, pH 7, and 303 K.

dx.doi.org/10.1021/la400789k | *Langmuir* 2013, 29, 7629−7641

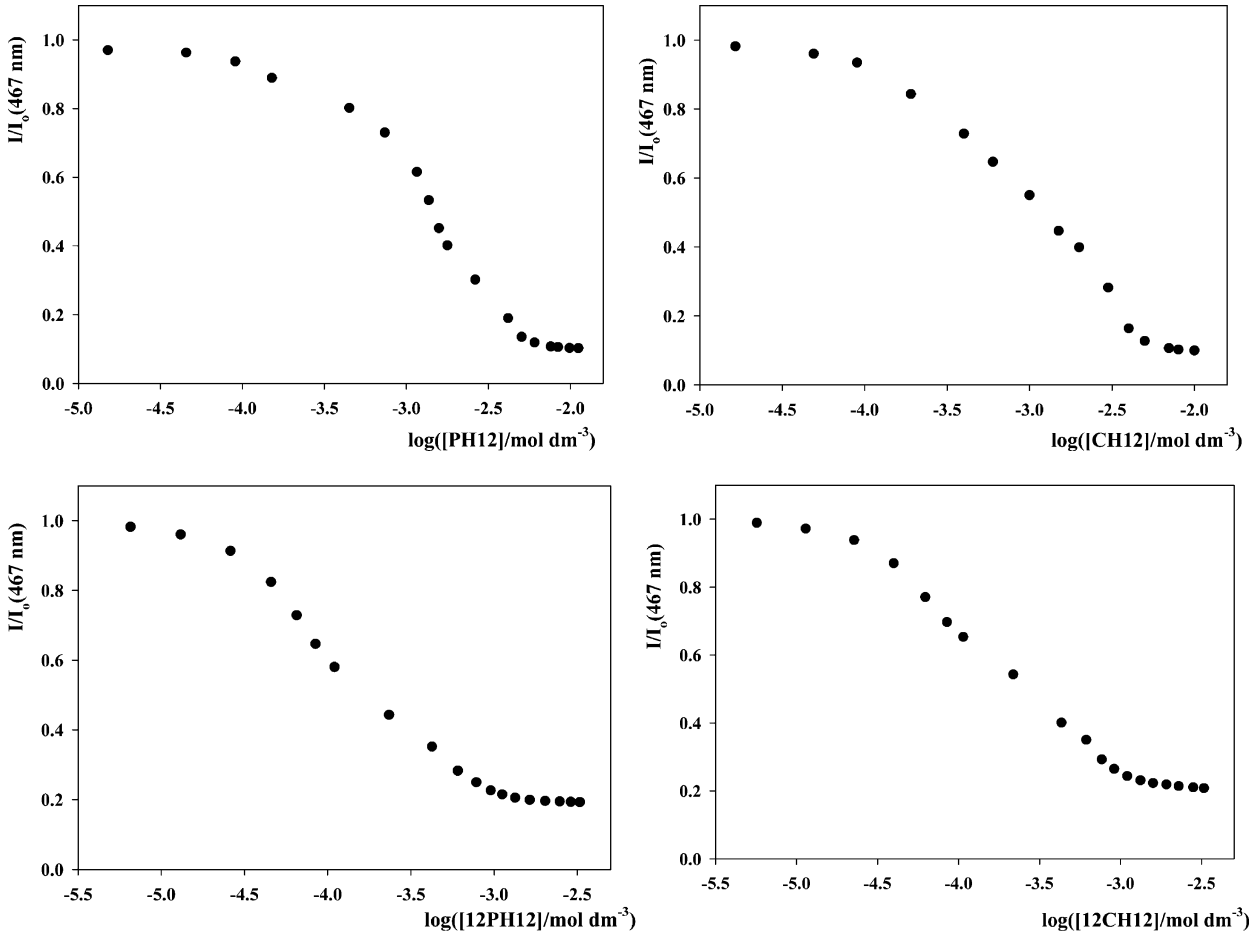

Figure 6. Relative fluorescence intensity of ANS (2×10^{-5} mol dm^{-3}) in the presence of 0.33 g/L BSA as a function of total surfactant concentration. I and I_o are the intensities in the presence and absence of a surfactant, respectively, at pH 7 and 303 K.

at 467 nm, respectively. Figure 6 shows an initial gradual decrease in I/I_o at a low surfactant concentration.

This diminution can be explained by the competition of the surfactants with ANS molecules for the binding sites of the protein, displacing them to different environments where the quantum yield is reduced. Subsequently, a steeper decrease in I/I_o is observed when the surfactant concentration increases, which corresponds to the cooperative binding of surfactant molecules to the protein. Here, in addition to the displacement of ANS molecules from their binding sites, the gradual denaturation of the protein results in the exposure of the ANS binding sites to a more polar environment, where its quantum yield is diminished. Besides, some ANS molecules can be solubilized in surfactant micelle-like clusters formed on the protein, where their quantum yield is also low.[26] At high surfactant concentrations, I/I_o becomes independent of surfactant concentration. This indicates that the BSA–surfactant interactions are saturated, and a subsequent increase in surfactant concentration results in the formation of aggregates. Figure 6 shows that an increase in the number of hydrophobic chains as well as the substitution of a cyclohexyl ring with a phenyl ring, either in the headgroup of the single-chain surfactants or in the spacer of the dimeric ones, results in a steeper decrease in I/I_o. These observations are in agreement with the results shown in Figures 2 and 3.

Circular Dichroism. Circular dichroism (CD) measurements can be used to study changes in the secondary structure of BSA caused by the surfactants.[49] Figure 7 shows the CD spectra of the protein in the absence and presence of the surfactants investigated. The surfactants do not contribute to the CD signal in the range of 200–250 nm; thus, the observed CD spectrum is solely due to the peptide bonds of the protein. Native BSA exhibits two negative bands at 208 and 222 nm, characteristic of the α-helix structure. Alterations in ellipticity at 222 nm (θ_{222}) are useful for visualizing the variations in α-helix content.[17] Figure 7 shows that, in all cases, the addition of surfactant results in a diminution of θ_{222}, suggesting a decrease in the α-helix content as a result of the unfolding of BSA. This is attributed to the binding of the surfactant to the protein, which leads the BSA to an extended disordered structure with exposed hydrophobic residues. As a consequence, structures such as β-sheet and random coil appear.

ζ Potential. The net electrical charge of proteins is a parameter that strongly affects their physicochemical behavior in living organisms. Protein surfaces in an aqueous medium naturally become charged to form an electrical double layer. The most common surface charge-determining ions are H^+ and OH^-. In this case, the net surface charge is affected by the pH of the medium in which the protein is dispersed. Of particular importance is the pH value at which the protein surface is electrically neutral. At this pH, the electric repulsion between protein molecules is minimal. Hence, they can easily coagulate and precipitate.[50] The pH value at which the ζ potential, equivalent to the net charge of the molecule including bound ions, is zero is called the isoelectric point, IEP. The dependence of the BSA ζ potential on pH has been previously

dx.doi.org/10.1021/la400789k | Langmuir 2013, 29, 7629–7641

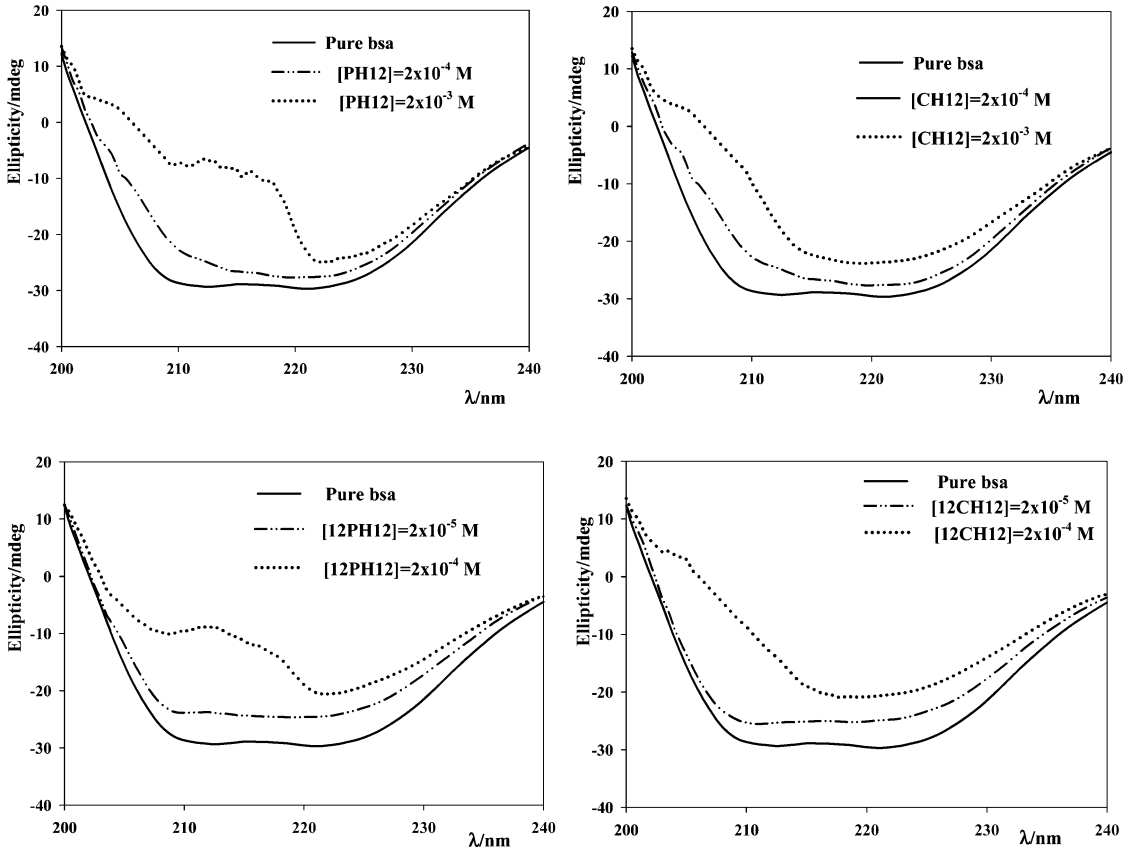

Figure 7. Circular dichroism spectra of BSA in the absence and presence of surfactants at 0.33 g/L BSA, pH 7, and 303 K.

investigated.[51,52] The ζ potential of BSA decreases from 50 mV, at pH 3, to −55 mV, at pH 10, for an ionic strength, I, of 10^{-3} mol dm^{-3}. For an I of 0.15 mol dm^{-3}, ζ goes from 30 mV, at pH 3, to −30 mV, at pH 10.[51] It was found that for BSA a zero value for the ζ potential was achieved at pH 5.1 and is independent of ionic strength.[51,52] It is interesting to point out that the uncompensated charge of BSA experimentally determined is much smaller than that theoretically predicted from the dissociation constant of the amino groups.[53] This was explained by considering the adsorption of counterions, and it is usually called the ion condensation phenomenon.[54] Because the level of adsorption of counterions increases with the ionic strength of the solution, the number of free charges for the protein diminishes with an increase in I.

Figure 8 shows the dependence of the BSA ζ potential on surfactant concentration at pH 7 (0.01 mol dm^{-3} phosphate buffer, I = 0.0108 mol dm^{-3}). One can see that, for all surfactants investigated, an increase in the surfactant concentration results in an increase in the ζ potential. This figure confirms that the positively charged surfactants studied in this work progressively bind to the protein, and as a result, the BSA charge goes from negative values to positive values when the surfactant concentration increases. At low surfactant concentrations, the ζ potential increases slowly. This region corresponds to the highly specific binding and noncooperative binding regions shown in Figure 4. Subsequently, an additional increase in the surfactant concentration causes a steeper increase in ζ, which can be due to the cooperative binding of the surfactant to the protein. Subsequently, ζ shows a tendency to reach a maximum. At this point, it is worth noting that the surfactant concentration contributes to the total ionic strength

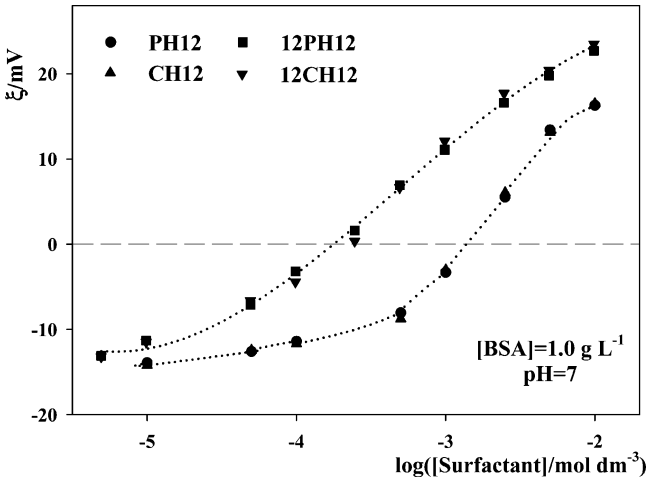

Figure 8. ζ potential of BSA as a function of surfactant concentration at pH 7 (0.01 mol dm^{-3} phosphate buffer), 1 g/L BSA, and 303 K.

of the solution. As monomers, they behave as strong electrolytes. When they form aggregates (in the solution or bound to the protein), a percentage of counterions, determined by the dissociation degree, remains in the aqueous bulk phase. At low surfactant concentrations, the contribution of the surfactant to I can be neglected under the working conditions, but this is not so at moderate or high surfactant concentrations. It is also important to note that the BSA concentration used in the ζ potential experiments was 1.0 g/L (see Experimental Section). Therefore, the C_1 values would be expected to be higher than in the case of 0.33 g/L BSA (as is observed by conductivity measurements for the single-chain surfactants

dx.doi.org/10.1021/la400789k | Langmuir 2013, 29, 7629−7641

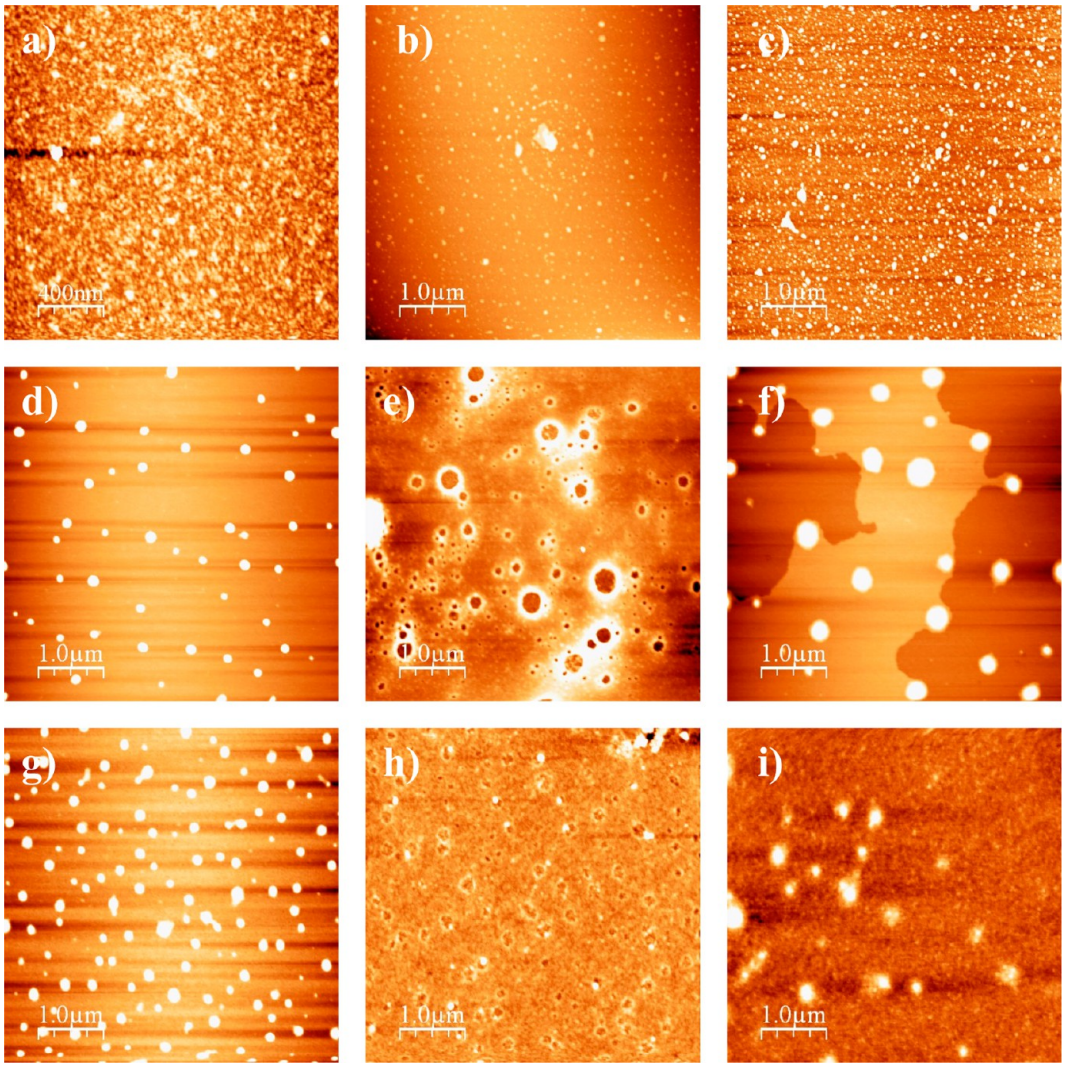

Figure 9. AFM topographic image of BSA/surfactant solutions in phosphate buffer (pH 7), adsorbed on $MgCl_2$-modified and nonmodified mica surfaces: (a) pure BSA (1.0 g/L), (b) 12CH12 (5×10^{-4} mol dm^{-3}), (c) PH12 (2×10^{-3} mol dm^{-3}), (d) 12CH12 (0.01 mol dm^{-3}), (e) 12CH12 (5×10^{-5} mol dm^{-3}) and BSA (1.0 g/L), (f) 12CH12 (0.01 mol dm^{-3}) and BSA (1.0 g/L), (g) PH12 (0.01 mol dm^{-3}), (h) PH12 (5×10^{-4} mol dm^{-3}) and BSA (1.0 g/L), and (i) PH12 (0.03 mol dm^{-3}) and BSA (1.0 g/L).

investigated). Nonetheless, the trend shown by ζ with a change in surfactant concentration is not expected to depend much on the protein concentration. In fact, Kun et al.[55] found a similar dependence of ζ on surfactant concentration for various BSA/cationic surfactant solutions at pH 7.4 and 5.0 g/L BSA.

Figure 8 shows that the dimeric surfactants increase the BSA charge more effectively than the single-chain surfactants. In fact, the single-chain surfactant concentration necessary to neutralize the protein charge is close to 10 times higher than that of the dimeric surfactants. These results indicate that an increase in the number of hydrophobic chains favors BSA−surfactant interactions. They also point out that protein−surfactant interactions are electrostatic as well as hydrophobic, as expected. If only electrostatic interactions would be operative, the surfactant concentration of the dimeric surfactant resulting in a ζ of 0 mV should be approximately one-half of that of the single-chain surfactant, and this is not the case.

An interesting feature of Figure 8 is that no effect of the ring nature on the increment in ζ when surfactant concentration increases is observed, for both single-chain and dimeric surfactants, in contrast with the fluorescence results. A plausible explanation is that fluorescence measurements mainly show the effect of surfactant binding on the Trp and Tyr residues, or their surroundings, whereas ζ potential measures the effect of surfactant binding on the charge of the protein. If the surfactants with phenyl rings have a stronger preference for binding in the vicinity of the Trp and Tyr residues (both residues have aromatic rings) than the surfactants with cyclohexyl rings (or alkyl groups), a more effective quenching of Trp and Tyr fluorescence emission would be found for the former than for the latter. The same reasoning can be applied to the changes in ANS fluorescence with an increase in surfactant concentration because ANS molecules compete for the protein binding sites with the surfactants. However, this does not necessarily mean that 12PH12 and PH12 associate with the BSA more effectively than 12CH12 and CH12, but that the binding sites of the surfactants with aromatic rings to the BSA are somewhat different from those of the surfactants without aromatic rings.

AFM Measurements. AFM has become a central tool in analyzing the formation, topography, structure, dynamics, and molecular actions of biological materials.[56] AFM imaging of

dx.doi.org/10.1021/la400789k | *Langmuir* 2013, 29, 7629−7641

BSA solutions adsorbed on mica solid supports has previously been obtained at different pH values.[57] Besides, it has been shown that the analysis of the obtained images of the surface topography by AFM can provide information about the action of various additives on proteins.[56,58] Nonetheless, it is worth noting that from these experiments information about the species adsorbed on mica is obtained and that they could be different from those present in the solution.

Figure 9 shows the AFM topographic images of BSA/surfactant solutions, at pH 7. As shown in Figure 8, at pH 7 (0.01 mol dm^{-3} phosphate buffer) BSA is negatively charged. Because at this pH the mica surface was also negatively charged,[57] it had to be functionalized with $MgCl_2$ for the BSA molecules to be adsorbed. The resulting AFM image is shown in Figure 9a, which is in agreement with the results obtained by Bashileva et al.[58] The BSA concentration used in all the experiments was the same as in the ζ potential measurements, 1.0 g/L, because it was necessary to know the charge of the protein to design the experiments. Nonetheless, AFM experiments with buffered BSA solutions adsorbed on $MgCl_2$-functionalized mica with 0.5 and 0.25 g/L protein were conducted, and the images obtained were similar to that shown in Figure 9a. No AFM experiments with 12PH12 were conducted because during the sample preparation the dimeric surfactant precipitated on the mica surface. Results corresponding to BSA/CH12 solutions are not included in Figure 9 because they are similar to those of BSA/PH12 solutions. Panels b and c of Figure 9 show the images obtained for 12CH12 (5×10^{-4} mol dm^{-3}) and PH12 (2×10^{-3} mol dm^{-3}) buffered solutions, at surfactant concentrations below the cmc, in the absence of protein. Under these conditions, surfactant molecules are present in the solution as monomers, which adsorb at the negatively charged mica surface. The observed size distribution could be due the adsorption of more than one surfactant molecule at the same, or close, surface sites. The elongated and large structures can be due to the formation of crusts during the drying process in the sample preparation. Panels d and g of Figure 9 show the images of 12CH12 (0.01 mol dm^{-3}) and PH12 (0.01 mol dm^{-3}) buffered solutions with no BSA. In the two cases, the surfactant concentration is above the cmc and nearly spherical micelles can be observed, together with surfactant monomers, adsorbed at the surface. Micelles adsorbed at surfaces have been previously visualized by using AFM.[59,60] Panels e and h of Figure 9 correspond to buffered BSA/12CH12 (5×10^{-5} mol dm^{-3}) and BSA/PH12 (5×10^{-4} mol dm^{-3}) solutions adsorbed at a $MgCl_2$-functionalized mica surface, respectively. Results in Figure 8 point out that for these surfactant concentrations the BSA charge remains negative (approximately −5.0 mV), and it was necessary to functionalize the mica for the adsorption to occur. No micelle formation was expected for these surfactant concentrations. Panels e and h of Figure 9 show the formation of craterlike structures, which are not present in the absence of BSA (see Figure 9b,c). They are larger for the dimeric than for the single-chain surfactant. These structures could be assigned to BSA−surfactant complexes. Panels f and i of Figure 9 are the images of BSA/12CH12 (0.01 mol dm^{-3}) and BSA/PH12 (0.03 mol dm^{-3}) solutions. For these surfactant concentrations, the functionalization of the mica surface was not necessary (see Figure 8). In Figure 9f, large globular structures are observed, which could be attributed to the formation of clusters of BSA-decorated surfactant aggregates[30] of different sizes, which are adsorbed at the mica surface. The size of some of the globules shown in Figure 9f is similar to the size of those in Figure 9d, which correspond to BSA-free surfactant micelles. No effect of ionic strength on the micellar size when comparing panels d and f of Figure 9 is expected because in both cases the surfactant concentration is 0.01 mol dm^{-3} and the phosphate buffer is present. In Figure 9i, the surfactant concentration studied was 0.03 mol dm^{-3}, to be sure that the surfactant concentration was higher than C_1 (the BSA concentration was 1.0 g/L). At this high surfactant concentration, the imaging resolution was bad. Nonetheless, one can see the presence of globular structures with a wide size distribution, some of them attached to each other and to the surface. They could also be attributed to the formation of clusters of BSA−surfactant decorated micelles. Free single-chain surfactant micelles are also present. Because the surfactant concentration corresponding to Figure 9d is lower than that corresponding to Figure 9i, the contribution of ionic strength to the aggregate size cannot be ruled out.

CONCLUDING REMARKS

The experimental results obtained in this work unambiguously show that the cationic single-chain and dimeric surfactants investigated bind to the BSA at pH 7. Fluorescence measurements indicate that the binding was cooperative. At low surfactant concentrations, the interactions are expected to be mainly electrostatic, and when the surfactant concentration increases, hydrophobic interactions are also operative. At high surfactant concentrations, BSA−surfactant interactions are saturated and a subsequent increase in surfactant concentration results in the formation of micelles. Because electrostatic as well as hydrophobic interactions are expected to be stronger for dimeric surfactants than for single-chain surfactants, the former are more efficient as protein denaturants than the latter. In the case of the surfactants with a phenyl ring, PH12 and 12PH12, $\pi-\pi$ interactions with protein residues with aromatic rings are also expected to be operative. As a consequence, surfactants with a phenyl ring reduce the intrinsic fluorescence of BSA more effectively, as well as that of the extrinsic probe ANS, when the surfactant concentration increases as compared to that caused by surfactants with a cyclohexyl ring. However, ζ potential values are not influenced when a cyclohexyl ring is substituted with a phenyl ring for both single-chain and dimeric surfactants, in contrast with the fluorescence results. A plausible explanation is that fluorescence measurements mainly show the effect of surfactant binding on the Trp and Tyr residues, or their surroundings, whereas the ζ potential measures the effect of the surfactant binding on the charge of the protein. That is, 12CH12 and CH12, can associate as efficiently as 12PH12 and PH12 with BSA, respectively, but the binding sites of the surfactants with aromatic rings to the BSA are somewhat different from those of the surfactants with no aromatic rings.

Finally, the AFM images show that, in the absence of protein, both the surfactant monomers and the micelles adsorb at the mica surface. When BSA is present in the solution, craterlike structures are observed for surfactant concentrations below C_1, which could be assigned to BSA−surfactant complexes. When the surfactant concentration is greater than C_1, globular structures are observed, and they were attributed to BSA-decorated surfactant micelles. For these high surfactant concentrations, free surfactant micelles are also observed.

dx.doi.org/10.1021/la400789k | Langmuir 2013, 29, 7629−7641

■ ASSOCIATED CONTENT

Supporting Information

Fluorescence spectra of BSA/ANS solutions and fluorescence spectra of ANS in BSA/surfactant solutions. This material is available free of charge via the Internet at http://pubs.acs.org.

■ AUTHOR INFORMATION

Corresponding Author

*E-mail: moya@us.es.

Notes

The authors declare no competing financial interest.

■ ACKNOWLEDGMENTS

This work was financed by the DGCYT (Grant BQU2009-07478), the FEDER funds, and Consejería de Innovación, Ciencia y Empresa de la Junta de Andalucía (FQM-274 and P07-FQM-03056). We thank Dr. Consuelo Cerrillos for her help with the AFM measurements.

■ REFERENCES

(1) Sulkowska, A.; Bojko, B.; Rownicka, J.; Sulkowski, W. Effect of urea on serum albumin complex with antithyroid drugs: A fluorescence study. *J. Mol. Struct.* **2003**, *651*, 237−243.

(2) Goddard, E. D.; Ananthapadmanabhan, K. P. *Interactions of surfactants with polymers and proteins*; CRC Press Inc.: London, 1992.

(3) Shah, A.; Bano, B. Spectroscopic studies on the interaction of bilirubin with liver cystatin. *Eur. Biophys. J.* **2011**, *40*, 175−180.

(4) Nemirovskiy, O. V.; Ramanathan, R.; Gross, M. L. Investigation of calcium-induced, noncovalent association of calmodulin with melittin by electrospray ionization mass spectrometry. *J. Am. Soc. Mass Spectrom.* **1997**, *8*, 809−812.

(5) Smalley, J. W.; Charalabou, P.; Hart, C. A.; Silver, J. Transmissible *Burkholderia cepacia* genomovar IIIA strains bind and convert monomeric iron(III) protoporphyrin IX into the M-oxo oligomeric form. *Microbiology* **2003**, *149*, 843−853.

(6) Wilcox, M. In *Poucher's perfumes, cosmetics and soaps*, 10th ed.; Butler, H., Ed.; Kluwer Academic Publishers: Dordrecht, The Netherlands, 2000; pp 453−465.

(7) McClements, D. J. *Food Emulsions: Principles, practice and techniques*, 2nd ed.; CRC Press: Boca Raton, FL, 2004.

(8) Jones, M. N. Surfactant interactions with biomembranes and proteins. *Chem. Soc. Rev.* **1992**, *21*, 127−136.

(9) Jones, M. N. In *Food polymers, gels and colloids*; Dikinson, E., Ed.; The Royal Society of Chemistry: Cambridge, U.K., 1991; pp 65−80.

(10) Mishra, M.; Muthuprasanna, P.; Prabha, K. S.; Rani, P. S.; Babu, I. A. S.; Chandiran, I. S.; Arunachalam, G.; Shalini, S. Basics and potential applications of surfactants: A review. *Int. J. PharmTech Res.* **2009**, *1*, 1354−1365.

(11) Jones, M. N. Surface activity of proteins. In *Chemical and physicochemical modifications*; Magdassi, S., Ed.; Marcel Dekker: New York, 1996; pp 237−284.

(12) Randolph, T. W.; Jones, L. S. Rational design of stable protein formulations. In *Theory and practice*; Carpenter, J. F., Manning, M., Eds.; Kluwer Academic/Plenum Publishers: New York, 2002; pp 159−175.

(13) Otzen, D. Protein-surfactant interactions. A tale of many states. *Biochim. Biophys. Acta* **2011**, *1814*, 562−591.

(14) Ge, Y.-S.; Tai, S.-X.; Xu, Z.-Q.; Lai, L.; Tian, F.-F.; Li, D.-W.; Jiang, F.-L.; Liu, Y.; Gao, Z.-N. Synthesis of three novel gemini surfactants and comparative studies of their assemble behavior in the presence of bovin serum albumin. *Langmuir* **2012**, *28*, 5913−5920.

(15) Wang, Y. S.; Guo, R.; Xi, J. Comparative studies of interactions of hemoglobin with single-chain and with gemini surfactants. *J. Colloid Interface Sci.* **2009**, *331*, 470−475.

(16) Wu, D.; Xu, G. Y.; Feng, Y. J.; Wang, Y. J.; Zhu, Y. Y. Comparative study on interaction of bovine serum albumin with dissymmetric and symmetric gemini surfactant by spectral method. *Colloid Polym. Sci.* **2009**, *287*, 225−230.

(17) Mir, M. A.; Khan, J. M.; Khan, R. H.; Rather, G. M.; Dar, A. A. Effect of spacer length of alkanediyl-α,ω-bis(dimethylcetylammonium bromide) gemini homologues on the interfacial and physicochemical properties of BSA. *Colloids Surf., B* **2011**, *77*, 54−59.

(18) Faustino, C. M. C.; Calado, A. R. T.; García-Rio, L. Gemini surfactant-protein interactions: Effect of pH, temperature, and surfactant stereochemistry. *Biomacromolecules* **2009**, *10*, 2508−2514.

(19) Menger, M.; Keiper, J. N. Gemini surfactants. *Angew. Chem., Int. Ed.* **2000**, *39*, 1906−1920.

(20) Zana, R. Dimeric (gemini) surfactants: Effects of the spacer group on the association behavior in aqueous solution. *J. Colloid Interface Sci.* **2002**, *248*, 203−220.

(21) Rosen, M. J.; Tracy, D. J. Gemini surfactants. *J. Surfactants Deterg.* **1998**, *1*, 547−554.

(22) Hait, S. K.; Moulik, S. P. Gemini surfactants. A distinct class of self-assembling molecules. *Curr. Sci.* **2002**, *82*, 1011−1111.

(23) Martín, V. I.; Rodríguez, A.; Graciani, M. M.; Robina, I.; Carmona, A.; Moyá, M. L. Physicochemical characterization of bromide mono- and dimeric surfactants with phenyl and cyclohexyl rings in the head groups. *J. Colloid Interface Sci.* **2011**, *363*, 284−294.

(24) Huang, B. X.; Kim, H. Y.; Dass, C. Probing three-dimensional structure of bovine serum albumin by chemical cross-linking and mass spectrometry. *J. Am. Soc. Mass Spectrom.* **2004**, *15*, 1237−1247.

(25) Cattoni, D. I.; Kaufman, S. B.; Flecha, F.; González, L. Kinetics and thermodynamics of the interaction of 1-anilino-naphthalene-8-sulfonate with proteins. *Biochim. Biophys. Acta* **2009**, *1794*, 1700−1708.

(26) Deleu, M.; Paquet, M.; Blecker, C. In *Encyclopedia of Surface and Colloid Science*; Hubbard, A. T., Ed.; Marcel Dekker: New York, 2002; p 5119.

(27) Almgren, M. Diffusion-influenced deactivation processes in the study of surfactant aggregates. *Adv. Colloid Interface Sci.* **1992**, *41*, 9−32.

(28) Wu, D.; Xu, G.; Zhang, H.; Mao, H.; Feng, Y. Interactions between proteins and cationic gemini surfactants. *Biomacromolecules* **2007**, *8*, 708−712.

(29) Horcas, I.; Fernández, R.; Gómez-Rodríguez, J. M.; Colchero, J.; Gómez-Herreo, J.; Baro, A. M. WSxM: A software fo scanning probe microscopy and a tool for anotechnolgy. *Rev. Sci. Instrum.* **2007**, *78*, 013705.

(30) Singh, T.; Bharmoria, P.; Morikawa, M.; Kimizuka, N.; Kumar, A. Ionic-liquids induced structural changes of bovine serum albumin in aqueous media: A detailed physicochemical and spectroscopic study. *J. Phys. Chem. B* **2012**, *116*, 11924−11935.

(31) Chakraborty, T.; Chakraborty, I.; Moulik, S. P.; Ghosh, S. Physicochemical and conformational studies on BSA-surfactant interaction in aqueous medium. *Langmuir* **2009**, *25*, 3062−3074.

(32) Ananthapadmanabhan, K. P. In *Interactions of Surfactants with Polymers and Proteins*; Goddard, E. D., Ananthapadmanabhan, K. P., Eds.; CRC Press, Inc.: London, 1993; Chapter 8.

(33) Lu, J. R.; Simister, E. A.; Lee, E. M.; Thomas, R. K. Direct determination by neutron reflection of the penetration of water into surfactant layers at the air/water interface. *Langmuir* **1992**, *8*, 1837−1844.

(34) Li, Z. X.; Lu, J. R.; Thomas, R. K. Neutron reflectivity studies of the adsorption of Aerosol-OT at the air/water interface: The surface excess. *Langmuir* **1997**, *13*, 3681−3685.

(35) Downer, A. D.; Eastoe, J.; Pitt, A. R.; Penforld, J.; Heenan, R. K. Adsorption and micellization of partially- and fully-fluorinated surfactants. *Colloids Surf., A* **1999**, *156*, 33−48.

(36) Eastoe, J.; Nave, S.; Downer, A.; Paul, A.; Rankin, A.; Tribe, K. Adsorption of ionic surfactants at the air-solution interface. *Langmuir* **2000**, *16*, 4511−4518.

(37) Madaeni, S. S.; Roshami, E. Spectroscopic investigation of the interaction of BSA with cationic surfactants. *Chem. Eng. Technol.* **2008**, *31*, 1265−1271.

(38) Salis, A.; Boström, M.; Medda, L.; Cugia, F.; Barse, B.; Parsons, D. F.; Ninham, B. W.; Monduzzi, M. Measurements and theoretical interpretation of points of zero charge/potential of BSA protein. *Langmuir* **2011**, *27*, 11597−11604.
(39) Bakshi, M. S.; Kaur, I. Benzylic and pyridinium groups controlled surfactant-polymer aggregates of mixed cationic micelles and anionic polyelectrolytes. *Colloid Polym. Sci.* **2004**, *282*, 476−485.
(40) Mata, J.; Varade, D.; Bahadur, P. Aggregation behavior of quaternary salt based cationic surfactants. *Thermochim. Acta* **2005**, *428*, 147−155.
(41) Prasad, M.; Moulik, S. P.; Palepu, R. Self-aggregation of binary mixtures of alkyltriphenylphosphonium bromides: A critical assessment in favor of more than one kind of micelle formation. *J. Colloid Interface Sci.* **2005**, *284*, 658−666.
(42) Li, Y.; Wang, X.; Wang, Y. Comparative study on the interactions of bovine serum albumin with gemini and single-chain surfactants. *J. Phys. Chem. B* **2006**, *110*, 8499−8505.
(43) Zhou, T.; Ao, M.; Liu, T.; Zhang, J. Interactions of bovine serum albumin with cationic imidazolinium surfactants and quaternary amonium gemini surfactants: Effects of surfactant architecture. *J. Colloid Interface Sci.* **2013**, *389*, 175−181.
(44) De, S.; Girigoswami, A.; Das, S. Fluorescence probing of albumin-surfactant interaction. *J. Colloid Interface Sci.* **2005**, *285*, 562−573.
(45) Pi, Y.; Shang, Y.; Peng, C.; Liu, H.; Hu, Y.; Jiang, J. Interactions between bovine serum albumin and gemini surfactants alkanedyl-α,ω-bis(dimethyldodecylammonium bromide). *Biopolymers* **2006**, *83*, 243−249.
(46) Poulli, K.; Chantzos, N.; Mousdis, G. A.; Georgiu, C. A. Synchronous fluorescence spectroscopy: Tool for monitoring thermally stressed edible oils. *J. Agric. Food Chem.* **2009**, *57*, 8194−8201.
(47) Kosower, E. M.; Kanety, H. Intramolecular donor−acceptor systems. 10. Multiple fluorescences from 8-(N-phenylamino)-1-naphthalenesulfonates. *J. Am. Chem. Soc.* **1983**, *105*, 6236−6243.
(48) Kirk, W.; Klimtchuk, E. Photophysics of ANS. III: Circular dichroism of ANS and anilinonaphthalene in I-FABP. *Biophys. Chem.* **2007**, *125*, 24−31.
(49) Sreerama, N.; Woody, R. W. Estimation of protein secondary structure from circular dichroism spectra: Comparison of CONTIN, SELCON, and CDSSTR methods with an expanded reference set. *Anal. Biochem.* **2000**, *287*, 252−260.
(50) Ninham, B. W.; Lo Nostro, P. Molecular forces and self-assembly. In *Colloid, nano sciences and biology*; Cambridge University Press: Cambridge, U.K., 2010.
(51) Salis, A.; Boström, M.; Medda, L.; Cugia, F.; Barse, B.; Parsons, D. F.; Niham, B.; Monduzzi, M. Measurements and theoretical interpretation of points of zero charge/potential of BSA protein. *Langmuir* **2011**, *27*, 11597−11604.
(52) Jachimska, B.; Wasilewska, M.; Adamczyk, Z. Characterization of globular protein solutions by dynamic light scattering, electrophoretic mobility, and viscosity measurements. *Langmuir* **2008**, *24*, 6866−6874.
(53) Rezwan, K.; Meier, L. P.; Rezwan, M.; Voros, J.; Gauckler, L. J. Bovin serum albumin adsorption onto colloidal Al_2O_3 particles; A new model based on ζ potential and UV-visible measurements. *Langmuir* **2004**, *20*, 10055−10061.
(54) Adamczyk, Z.; Bratek, A.; Jachimska, B.; Jasinski, T.; Warszynski, P. Structure of poly(acrylic acid) in electrolyte solutions determined from simulations and viscosity measurements. *J. Phys. Chem. B* **2006**, *110*, 22426−22435.
(55) Kun, R.; Kis, L.; Dekany, I. Hydrophobization of bovine serum albumin with cationic surfactants with different hydrophobic chain length. *Colloid Surf., B* **2010**, *79*, 61−68.
(56) Cohen, S. R.; Bitler, A. Use of AFM in bio-related systems. *Curr. Opin. Colloid Interface Sci.* **2008**, *13*, 316−325.
(57) Demaneche, S.; Chapel, P.; Monrozier, L. J.; Quiquampoix, H. Dissimilar pH-dependent adsorption fetures of bovine serum albumin and chymotrypsin on mica probed by AFM. *Colloid Surf., B* **2009**, *70*, 226−231.
(58) Balasheva, K.; Callisen, T. H.; Svendsen, A.; Bjornholm, T. Savinase action on bovine serum albumin (BSA) monolayers demonstrated with measurements at the air-water interface and atomic force microscopy (AFM) imaging. *Colloid Surf., B* **2011**, *88*, 582−586.
(59) Aytun, T.; Mutaf, O. M.; el-Atwani, J.; Ow-Yang, C. W. Nanoscale composition mapping of segregation in micelles with tapping-mode atomic force microscopy. *Langmuir* **2008**, *24*, 14183−14187.
(60) Zhang, X.; Wang, Y.; Wang, W. Salt indiced aggregation of polyelectrolyte-amphiphilic dendron complexes in THF solutions. *Langmuir* **2009**, *25*, 2075−2080.